Hopping transport in the precursor glasses of the superconducting system Bi-Sr-Ca-Cu-O

1990 J. Phys.: Condens. Matter 2 649

(http://iopscience.iop.org/0953-8984/2/3/013)

J. Phys.: Condens. Matter 2 (1990) 649–660. Printed in the UK

Hopping transport in the precursor glasses of the superconducting system Bi–Sr–Ca–Cu–O

Aswini Ghosh and D Chakravorty
Indian Association for the Cultivation of Science, Jadavpur, Calcutta 700032, India

Received 26 July 1989

Abstract. The first measurement is reported for the electrical properties of the precursor glasses in the high-temperature superconducting system Bi–Sr–Ca–Cu–O. The phonon-assisted hopping of small polarons is consistent with the DC conductivity in the high temperature region; however, at lower temperatures a variable range hopping mechanism dominates the conductivity. The correlated barrier hopping model is consistent with the temperature and frequency dependence of the AC conductivity and its frequency exponent.

1. Introduction

The discovery of high-temperature superconductivity in the La–Ba–Cu–O system by Bednorz and Muller (1986) has been followed by the observation of higher critical temperatures in the systems Y–Ba–Cu–O, Bi–Sr–Ca–Cu–O and Tl–Ba–Ca–Cu–O respectively (Wu *et al* 1987, Maeda *et al* 1988, Sheng and Herman 1988). The Bi–Sr–Ca–Cu–O system generally consists of a few superconducting phases with different critical temperatures, the formation of these phases being dependent on the processing conditions (Tarascon *et al* 1988). Maeda *et al* (1988) reported that the compositions $Bi_1Sr_1Ca_1Cu_2O_{5.5-x}$ and $Bi_4Sr_3Ca_3Cu_4O_{16-x}$ have critical temperatures of 105 K and 85 K, respectively. Recently a glass–ceramic route of preparing high-temperature superconductors has been explored in this system (Zheng and Mackenzie 1988, Komatsu *et al* 1988). This leads to the possibility of drawing the glass in the form of wires and subsequently developing superconducting properties in them by subjecting these to a suitable heat-treatment schedule. Apart from a possible technological benefit, studies on the precursor glass and the subsequent crystallisation process may shed some light on the role of the different valence states of copper on the superconducting behaviour of these compounds. As part of a wider investigation, we have studied the electrical properties of the precursor glass in the Bi–Sr–Ca–Cu–O system. The results are reported here and are examined in terms of existing theories.

2. Experiment

Glass samples of three compositions (as given in table 1) were prepared from reagent grade bismuth oxide, strontium carbonate, calcium carbonate and copper carbonate. The chemicals were mixed in the Bi: Sr: Ca: Cu ratios, = 1:1:1:2, 2:2:2:3 and 4:3:3:4,

0953-8984/90/030649 + 12 $03.50

Table 1. Glass composition, density, transition-metal concentration and related parameters.

Glass composition	Density (gm cm^{-3})	Total copper ion concentration (10^{22} cm^{-3})	Cu^{2+} ion concentration (10^{19} cm^{-3})	C	R (Å)
$Bi_1Sr_1Ca_1Cu_2O_{5.5-x}$	6.07	1.12	2.65	0.97	4.47
$Bi_2Sr_2Ca_2Cu_3O_{10-x}$	5.89	1.07	3.96	0.96	4.53
$Bi_4Sr_3Ca_3Cu_4O_{16-x}$	5.75	0.73	4.00	0.94	5.12

respectively. A 15 g batch of each composition was melted at 1000 °C for two hours in air in alumina crucible and then the melt was quenched by pressing the molten mass between two brass plates. Samples of thickness ~1 mm with dark black colour were obtained. The amorphous nature of the samples was confirmed from x-ray diffraction patterns (using a Philips PW 1050 instrument). The density of the samples (table 1) was measured using Archimedes' principle.

For electrical measurements, disc-shaped samples of diameter ~8 mm were cut and polished. Gold electrodes were deposited on both surfaces of the disc-shaped samples by vacuum evaporation. The DC electrical conductivity of the samples was measured using a Keithley 617 programmable electrometer. The absence of barrier layers at the contacts was ascertained by studying the I–V characteristics which were found to be linear. The AC measurements were carried out using a General Radio (Model GR-1615A) capacitance bridge for frequencies between 10^2 and 10^5 Hz in a three-terminal arrangement. The sample holder was inserted in a cryogenic unit and measurements were made in the temperature range 80–420 K with a stability of ±0.5 K. The concentrations of the total Cu ions present in the glass matrices were estimated from atomic absorption spectroscopy (Varian AA1475). The concentrations of the Cu^{2+} ions were obtained from the ESR spectra (Varian E112) taken at room temperature. A spectrum of $CuSO_4 . 5H_2O$ was used as a standard. The Cu^{2+} concentrations are ~10^{19} cm^{-3} (table 1), much smaller than the total Cu concentrations (~10^{22} cm^{-3}). This fact indicates that most of the Cu^{2+} ions were reduced to Cu^{+} ions during the glass melting process. We could not find the presence of any Cu^{3+} ions in the ESR spectra. The average site separation R was estimated from the total copper ion concentrations and is shown in table 1. The ratio C of the concentration of the reduced copper ions to that of the total copper ions is also shown in table 1.

3. Results and discussion

3.1. DC conductivity

A semi-logarithmic plot of the DC conductivity as a function of inverse temperature is shown in figure 1. It is evident from the figure that the DC conductivity is linear with inverse temperature above 250 K, so the activation energy is constant in the high temperature region. However, below 250 K the conductivity varies smoothly with temperature, indicating a temperature-dependent activation energy. This type of behaviour is typical of small polaron-hopping conduction (Mott 1968, Austin and Mott 1969, Schnakenberg 1968, Emin and Holstein 1969).

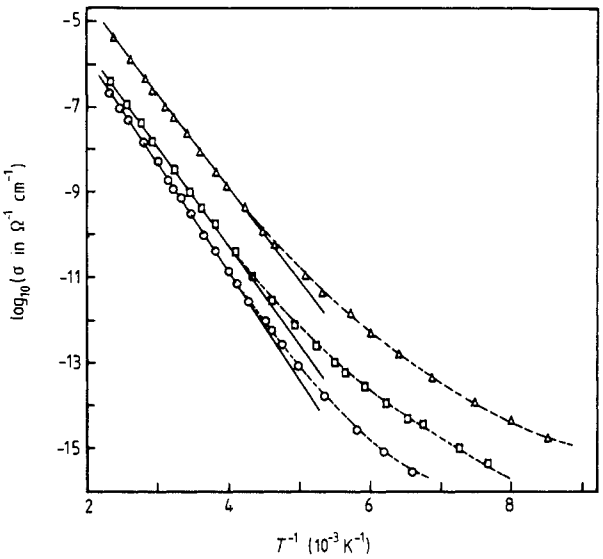

Figure 1. Temperature dependence of the DC conductivity for different glass compositions:
△, $Bi_1Sr_1Ca_1Cu_2O_{5.5-x}$;
□, $Bi_2Sr_2Ca_2Cu_3O_{10-x}$;
○, $Bi_4Sr_3Ca_3Cu_4O_{16-x}$.
The full lines are the theoretical fits to equation (1).

Table 2. Transport parameters for different Bi–Sr–Ca–Cu–O glasses (see text for definitions).

Glass composition	W (eV)	ν_0 (10^{13} s^{-1})	α (Å)$^{-1}$	r_p (Å) From (5)	r_p (Å) From (4)
$Bi_1Sr_1Ca_1Cu_2O_{5.5-x}$	0.46	2.0	0.28	1.80	1.98
$Bi_2Sr_2Ca_2Cu_3O_{10-x}$	0.48	1.0	0.36	1.83	2.10
$Bi_4Sr_3Ca_3Cu_4O_{16-x}$	0.51	1.0	0.37	2.06	2.26

The DC conductivity in the high temperature region ($T > 250$ K) can be fitted to the phonon-assisted hopping conductivity of small polarons derived by Mott (1968) in the non-adiabatic approximation:

$$\sigma = \nu_0 e^2[C(1-C)/kTR]\exp(-2\alpha R)\exp(-W/kT) \tag{1}$$

where ν_0 is the optical phonon frequency, α^{-1} the radius of wave function localisation, R the average hopping distance, C the ratio of Cu^+ ion concentration to the total Cu ion concentration and W the activation energy. Austin and Mott (1969) showed that

$$W = \begin{cases} W_h + W_d/2 & T > \theta_D/2 \\ W_d & T < \theta_D/4 \end{cases} \tag{2}$$

where W_h is the hopping energy, W_d the disorder energy arising from the energy difference of the neighbouring sites and θ_D the Debye temperature. The best fits (figure 1) are obtained for the values of ν_0, α and W shown in table 2. In the calculation the values of average Cu ion spacing (table 1) are used for R. The values of α indicate strong localisation in the Bi–Sr–Ca–Cu–O glasses (Mott and Davis 1979). The values of ν_0 are close to the phonon frequencies estimated from the infrared spectra of these glasses (Ghosh and Chakravorty 1989). The Debye temperature given by $\theta_D = h\nu_0/k$ is estimated to be of the order of 480 K. Assuming the high temperature activation energy W

to be close to the hopping energy W_h (Austin and Mott 1969), the electron–phonon coupling parameter given by $\gamma = 2W_h/h\nu_0$ is estimated to be ~11, which implies the presence of strong electron–phonon interaction and the formation of small polarons in the Bi–Sr–Ca–Cu–O glasses (Austin and Mott 1969).

Two methods of calculating the polaron binding energy W_p have been suggested. The most general expression for W_p has been given by Holstein (1959) as

$$W_p = \frac{1}{2N}\sum_q |\gamma_q|^2 h\nu_q \tag{3}$$

where $|\gamma_q|^2$ is the electron–phonon coupling constant and ν_q is the frequency of optical phonons of wavenumber q and N is the site concentration. Austin and Mott (1969) have derived a more direct expression for W_p, namely

$$W_p = e^2/2\varepsilon_p r_p \tag{4}$$

where r_p is the small polaron radius and ε_p is an effective dielectric constant given by $1/\varepsilon_p = 1/\varepsilon_\infty - 1/\varepsilon_s$ where ε_∞ and ε_s are the high-frequency and static dielectric constants, respectively. Bogomolov *et al* (1968) have shown that an expression of the form of (4) can be derived from (3) for the case of a non-dispersive system of frequency ν_0. The polaron radius is given by

$$r_p = \tfrac{1}{2}(\pi/6)^{1/3}R. \tag{5}$$

The value of the polaron radius calculated from (5) using the average site spacing (table 1) as an estimate for R is shown in table 2. An experimental estimate of the polaron radius may be obtained from (4) assuming $W \simeq W_h = W_p/2$ (Austin and Mott 1969). The values obtained are also shown in table 2. The values of ε_p used in the calculation are obtained from the Cole–Cole plot of the real and imaginary dielectric constants. It may be noted from table 2 that agreement between the theoretical and experimental estimates of r_p may be regarded as satisfactory considering the fact that the possible effect of disorder has been neglected in the above calculation. The small values of the polaron radii suggests that the polarons are highly localised.

The nature of the hopping mechanism in the high-temperature region can be determined from Holstein's condition (Holstein 1959, Emin and Holstein 1969). The polaron band width J should satisfy the relation

$$J \gtrless (2kTW_h/\pi)^{1/4}(h\nu_0/\pi)^{1/2} \tag{6}$$

where $>$ is for adiabatic hopping and $<$ for non-adiabatic hopping mechanisms, the condition for the existence of a small polaron being $J < W_h/3$. The limiting value of J calculated from the right-hand side of (6) at 400 K is ~0.04 eV. In the calculation the estimate of ν_0 from the electrical data has been used and the high-temperature activation energy has been assumed to be the polaron hopping energy. Since $W_h/3 \simeq 0.18$ eV, the condition for the formation of a small polaron is satisfied. An estimate of J can be made from the following relation (Mott and Davis 1979):

$$J \sim e^3[N(E_F)/\varepsilon_p^3]^{1/2}. \tag{7}$$

Using the values of $N(E_F)$ estimated later from the variable-range hopping analysis, equation (7) yields $J \sim 0.07$ eV. Therefore, the non-adiabatic hopping theory may be the most appropriate to describe polaronic conduction in the Bi–Sr–Ca–Cu–O glasses.

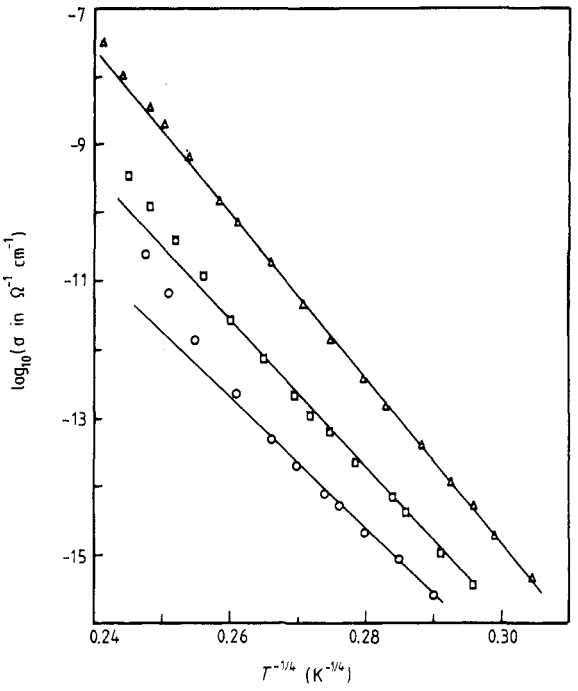

Figure 2. DC conductivity versus $T^{-1/4}$ for different glass compositions. The full lines are the theoretical fits to equation (8) corresponding to variable-range hopping.

Table 3. Density of states at the Fermi level and reciprocal radius of localisation from the variable range analysis.

Glass composition	α (Å)$^{-1}$	$N(E_F)$ (10^{18}eV^{-1}cm^{-3})
$Bi_1Sr_1Ca_1Cu_2O_{5.5-x}$	0.30	1
$Bi_2Sr_2Ca_2Cu_3O_{10-x}$	0.35	3
$Bi_4Sr_3Ca_3Cu_4O_{16-x}$	0.36	4

At low temperatures, where the polaron binding energy is small and the static disorder energy of the system plays a dominant role in the conduction process, Mott (1969) has suggested a variable-range hopping mechanism. The conductivity for the variable range hopping is given by

$$\sigma = A \exp(-B/T^{1/4}) \tag{8a}$$

where A and B are constants, and B is given by

$$B = 2.1[\alpha^3/kN(E_F)]^{1/4} \tag{8b}$$

where $N(E_F)$ is the density of states at the Fermi level.

A plot of log σ versus $T^{-1/4}$ for the present glasses is shown in figure 2, which suggests that the variable-range hopping mechanism may be valid in these glass systems below 180 K. Equation (8*a*) is fitted in figure 2 to the experimental data using α and $N(E_F)$ as variable parameters. The values of α and $N(E_F)$ obtained by the least-squares fitting are shown in table 3. These values are reasonable for localised states (Mott and Davis 1979).

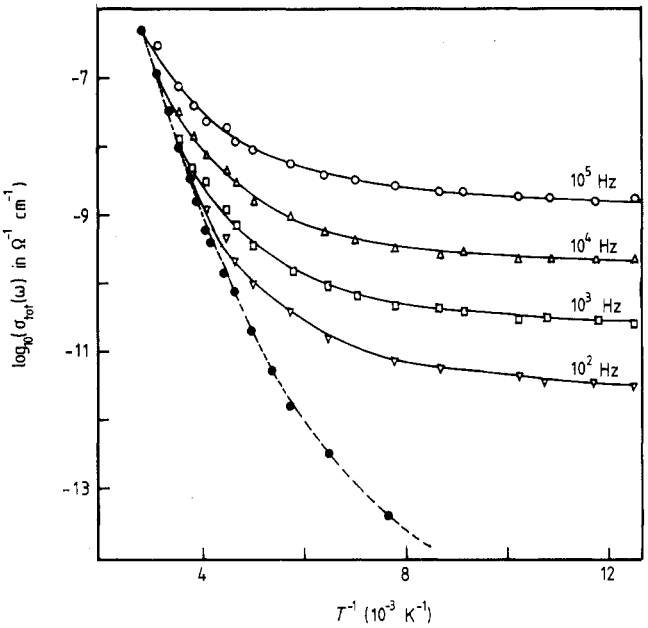

Figure 3. Temperature dependence of the total AC conductivity for $Bi_1Sr_1Ca_1Cu_2O_{5.5-x}$ glass at different frequencies. The full curves are theoretical fits to AC conductivity given by the CBH model (equation (13*b*)) plus the DC conductivity. The broken curve corresponds to the DC conductivity.

It may be noted that the values of α are similar to those estimated from the high temperature electrical data.

3.2. AC conductivity

The temperature dependence of the measured total conductivity $\sigma_{tot}(\omega)$ is shown in figure 3 as a function of frequency for one glass composition, along with the DC conductivity. It is already clear from the figure that the DC contribution is significant at high temperatures and low frequencies, while the frequency-dependent term dominates at low temperature and high frequencies. Similar behaviour is also observed for the other glass compositions.

The measured total conductivity $\sigma_{tot}(\omega)$ at angular frequency ω can be written as

$$\sigma_{tot}(\omega) = \sigma(\omega) + \sigma_{DC} \tag{9}$$

where σ_{DC} and $\sigma(\omega)$ are the DC and frequency-dependent AC conductivities respectively, and it is tacitly assumed that the DC and AC conductivities arise from completely different processes. However, when DC and AC conductivities are due to the same process and σ_{DC} is simply $\sigma(\omega)$ in the limit $\omega \rightarrow 0$, the separation given by (9) is no longer useful.

In many amorphous semiconductors and insulators (Mott and Davis 1979) the variation of AC conductivity with frequency invariably has the form

$$\sigma(\omega) = A\omega^s \tag{10}$$

where A is a constant dependent on temperature and s is a frequency exponent, generally $\leqslant 1$.

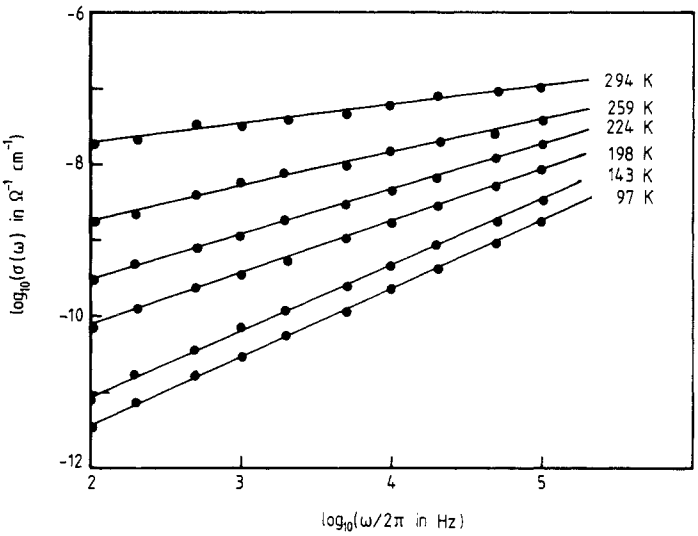

Figure 4. Variation of $\sigma(\omega) = \sigma_{tot}(\omega) - \sigma_{DC}$ as a function of frequency at different temperatures for the $Bi_1Sr_1Ca_1Cu_2O_{5.5-x}$ glass.

The frequency dependence of $\sigma(\omega)$ obtained by subtracting the DC conductivity from the measured total conductivity at various temperatures is shown in figure 4, for one glass composition. As is shown, the dependence follows the relation (10) well. The full lines in figure 4 are the straight-line fits obtained by the least-squares fitting procedure. The estimated frequency exponent s is shown in figure 5 as a function of temperature. It is observed that s decreases smoothly with increasing temperature. No frequency dependence of s is observed in the investigated frequency range.

Many different theories (Long 1982, Elliott 1987) for AC conduction in amorphous semiconductors have been proposed to account for the frequency and temperature dependence of $\sigma(\omega)$ and s. It is commonly assumed that the pair approximation holds, namely that dielectric loss occurs because the carrier motion is considered to be localised within pairs of sites. In essence, two distinct processes have been proposed for the relaxation mechanism, namely quantum mechanical tunnelling through the barrier separating two equilibrium positions and classical hopping of a carrier over the barrier, or some combination or variant of the two, and it is variously assumed that electrons (or polarons) or atoms are the carriers responsible for the dielectric loss. In what follows the data presented for the Bi–Sr–Ca–Cu–O glass are analysed on the basis of these models.

3.2.1. Quantum mechanical tunnelling (QMT) model. Several authors (Austin and Mott 1969, Pollak and Geballe 1961, Pollak 1965, 1971) have evaluated, within the pair approximation, the AC conductivity for single electron motion undergoing QMT and obtained the following expression for the AC conductivity:

$$\sigma(\omega) = \tfrac{1}{8}\pi e^2 kT[N(E_F)]^2 \alpha^{-5} \omega \ln^4(1/\omega\tau_0) \tag{11a}$$

where τ_0 is a characteristic relaxation time (of the order of the inverse phonon frequency). The frequency exponent s in this model is given by

$$s = 1 - 4/\ln(1/\omega\tau_0). \tag{11b}$$

Thus for the QMT model the AC conductivity is linearly dependent on temperature

and the frequency exponent is temperature independent. For typical values of the parameters, namely $\tau_0 \simeq 10^{-13}$ s and $\omega = 10^4\ s^{-1}$, a value of $s \simeq 0.81$ is deduced from (11*b*). However, it can be clearly seen from figure 5 that the general trend for s is to decrease with increasing temperature, thereby conflicting with the predictions of the simple QMT model. A temperature-dependent frequency exponent s can be obtained within the framework of the QMT model by assuming that the carriers form non-overlapping small polarons (Elliott 1977). In this case, however, the frequency exponent increases with increasing temperature, again in marked disagreement with the experimental data. The simple QMT model also predicts that s should decrease appreciably with increasing frequency. No such variation is observed for the present glasses.

In addition, the AC conductivity of the present glasses shows a temperature dependence of the order of $T^{1.25}$ at lower temperatures which is also inconsistent with the QMT model ((11*a*)). For these reasons, the QMT model, both for ordinary carriers and for non-overlapping small polarons, is inappropriate as a description of our data for the Bi–Sr–Ca–Cu–O glasses.

3.2.2. Overlapping large polaron tunnelling (OLPT) model. Long (1982) has proposed a mechanism for polaron tunnelling in which large polaron wells of the two sites overlap, thereby reducing the polaron hopping energy (Austin and Mott 1969)

$$W_h = W_{h0}(1 - r_0/R) \tag{12a}$$

where W_h is the polaron hopping energy, r_0 is the radius of the large polaron and W_{h0} is given by

$$W_{h0} = e^2/4\varepsilon_p r_0. \tag{12b}$$

The AC conductivity in this model (Long 1982) is given by

$$\sigma(\omega) = (\pi^4/12)e^2k^2T^2[N(E_F)]^2\ \omega R_\omega^4/(2\alpha kT + W_{h0}r_0/R_\omega^2). \tag{12c}$$

The hopping length R_ω is determined by quadratic equation

$$(R'_\omega)^2 + [W_{h0}/kT + \ln(\omega\tau_0)]R'_\omega - W_{h0}r'_0/kT = 0 \tag{12d}$$

where $R'_\omega = 2\alpha R_\omega$ and $r'_0 = 2\alpha r_0$.

The frequency exponent s in the OLPT model has been shown to be given by

$$s = 1 - (8\alpha R_\omega + 6W_{h0}r_0/kTR_\omega)/(2\alpha R_\omega + W_{h0}r_0/kTR_\omega)^2 \tag{12e}$$

Thus the OLPT model predicts that s should decrease from unity with increasing temperature. For large values of r'_0, s continues to decrease with increasing temperature, eventually tending to the value of s predicted by the simple QMT model, whereas for small values of r'_0, s exhibits a minimum at a certain temperature and subsequently increases in a manner similar to that exhibited by the small polaron QMT model.

At first sight it thus appears that the OLPT model might be a possible candidate theory to explain the data presented here, because the experimental values of s show a decrease with increasing temperature (figure 5). The theoretical curves for s (equation 12*e*) plotted versus kT/W_{h0} are shown in figure 6 as a function of r'_0. The experimental data for s are also plotted in the same figure rescaling the temperature axis. The fit to the low-temperature data only are obtained for the values of W_{h0} shown in table 4. These values of W_{h0} are used in (12*a*) to evaluate the polaron radius (table 4). It may be noted that the polaron radii, being smaller than the average intersite separation, are inconsistent with the basic premise of the OLPT model.

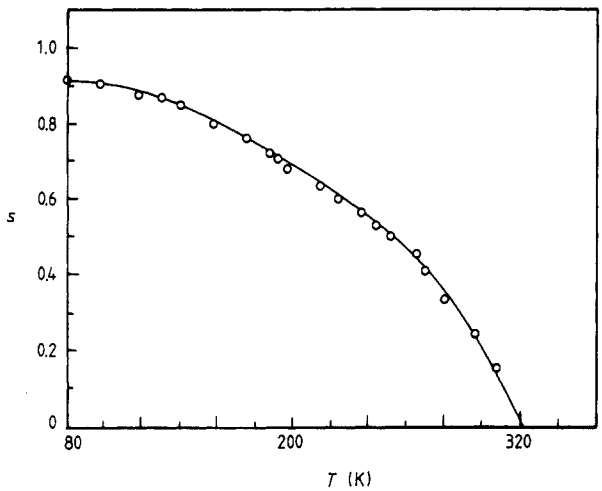

Figure 5. Temperature dependence of the frequency exponent s for the $Bi_1Sr_1Ca_1Cu_2O_{5.5-x}$ glass. The full curve in the figure is calculated using the CBH model (equation (13*d*)) assuming a frequency of 10 kHz.

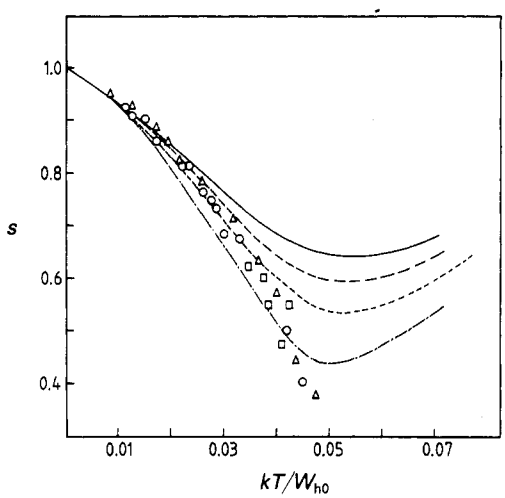

Figure 6. Variation of s as a function of kT/W_{h0} for different glass compositions: △, $Bi_1Sr_1Ca_1Cu_2O_{5.5-x}$; □, $Bi_2Sr_2Ca_2Cu_3O_{10-x}$; ○, $Bi_4Sr_3Ca_3Cu_4O_{16-x}$. The curves are drawn from equation (12*e*) for the following r_0' values assuming $\ln(\omega\tau_0) = -20$: —·—, $r_0' = 1.0$; – – –, $r_0' = 1.5$; ———, $r_0' = 2.0$; ———, $r_0' = 2.5$.

Table 4. Large-polaron radius obtained from the OLPT model.

Glass composition	W_{h0} (eV)	r_0'	r_0 (Å)
$Bi_1Sr_1Ca_1Cu_2O_{5.5-x}$	0.60	1.5	1.04
$Bi_2Sr_2Ca_2Cu_3O_{10-x}$	0.73	2.0	1.55
$Bi_4Sr_3Ca_3Cu_4O_{16-x}$	0.90	2.5	2.28

Table 5. Relaxation time and maximum barrier height obtained from the CBH model.

Glass composition	τ_0 (10^{-13} s)	W_m (eV)
$Bi_1Sr_1Ca_1Cu_2O_{5.5-x}$	50	0.63
$Bi_2Sr_2Ca_2Cu_3O_{10-x}$	10	0.77
$Bi_4Sr_3Ca_3Cu_4O_{16-x}$	8	0.90

However, there are several features which suggest that the OLPT model is unlikely to be the mechanism for AC conduction for the present glass system. Firstly no sign of a minimum is observed in the experimental plots of s versus T as is predicted by the model (figures 6 and 5, equation (12*e*)). Secondly the OLPT model (12*c*) predicts a considerably stronger temperature dependence of $\sigma(\omega)$ in the temperature regime where the frequency exponent s is a decreasing function of frequency than that observed experimentally. The functional form of the temperature dependence of $\sigma(\omega)$ as predicted by (12*c*) is complicated and cannot be simply expressed as $\sigma(\omega) \sim T^n$ with n constant over a wide temperature range. Nevertheless at low temperatures ($kT/W_{h0} < 0.04$) the hopping length R_ω has an approximate temperature dependence of $R_\omega \sim T^{1.25}$ and hence $\sigma(\omega) \sim T^6$ for the uncorrelated case. This is obviously at variance with the much weaker temperature dependence exhibited by the low-temperature data of the present work (figure 3) and even if the correlated form (Elliott 1987) of the OLPT is used the dependence is predicted to decrease only to $\sigma(\omega) \sim T^4$.

3.2.3. Correlated-barrier-hopping (CBH) model. A model for AC conduction which correlates the relaxation variable W with the intersite separation R has been developed initially by Pike (1972) for single electron hopping and extended by Elliott (1977, 1987) for two electrons hopping simultaneously. For neighbouring sites at a separation R the Coulomb wells overlap, resulting in a lowering of the effective barrier height from W_m to a value W, which for the two-electron hopping is given by

$$W = W_m - 2e^2/\pi\varepsilon\varepsilon_0 R \tag{13a}$$

where ε is the dielectric constant of the material and ε_0 that of free space. The AC conductivity in this CBH model in the narrow-band limit is given by

$$\sigma(\omega) = (\pi^3/12)N^2\varepsilon\varepsilon_0\omega R_\omega^6 \tag{13b}$$

where N is the concentration of pair sites and the hopping distance R_ω is given by

$$R_\omega = 2e^2/\pi\varepsilon\varepsilon_0[W_m + kT\ln(\omega\tau_0)]. \tag{13c}$$

The frequency exponent s for this model is given by

$$s = 1 - 6kT/[W_m + kT\ln(\omega\tau_0)]. \tag{13d}$$

Thus, in the CBH model, a temperature dependent frequency exponent s is predicted with s increasing towards unity as $T \to 0$ K and therefore it might be a possible contending theory for the AC conduction in the present glass system.

A critical test for the CBH model comes from the temperature dependences of $\sigma(\omega)$ and s. Fits of (13*d*) to the experimental data are shown in figure 5 as a function of temperature using W_m and τ_0 as variable parameters. The values of W_m and τ_0 obtained by the least-squares fitting procedure are shown in table 5. In the fitting procedure a

fixed frequency ($\omega = 10^4\ s^{-1}$) is assumed for all glass compositions. In figure 3, the measured total conductivity $\sigma_{tot}(\omega)$ is also fitted to the AC conductivity $\sigma(\omega)$ calculated from the CBH model (13*b*) using the same value of W_m and τ_0 plus the measured value of the DC conductivity σ_{DC}. It is observed that these fits appear to be reasonable over the entire measured temperature range. The CBH model therefore predicts the temperature dependence of both the AC conductivity and its frequency exponent. It may be noted that the values of τ_0 obtained from the fitting procedure are higher than that expected for the typical inverse phonon frequency ν_0. Such a discrepancy is however not unexpected when lattice relaxation effects (Elliott 1987) are important, as we believe to be the case here.

4. Conclusions

The DC conductivity of the Bi–Sr–Ca–Cu–O glasses in the high-temperature region is consistent with the phonon-assisted hopping of small polarons in the non-adiabatic regime, while at lower temperatures a variable-range hopping mechanism dominates the DC conductivity. The temperature dependence of the AC conductivity and its frequency exponent are consistent with the predictions of the correlated barrier hopping model over the entire temperature range of measurements. The quantum-mechanical tunnelling models of ordinary carriers, small polarons and overlapping large polarons cannot predict the observed data.

References

Austin I G and Mott N F 1969 *Adv. Phys.* **18** 41
Bednorz J G and Muller A 1986 *Z. Phys.* B **64** 189
Bogomolov V N, Kudinov E K and Firsov Y A 1968 *Sov. Phys.–Solid State* **9** 2502
Elliott S R 1977 *Phil. Mag.* **36** 1291
—— 1978 *Phil. Mag.* B **37** 553
—— 1987 *Adv. Phys.* **36** 135
Emin D and Holstein T 1969 *Ann. Phys., NY* **53** 439
Friedman L and Holstein T 1963 *Ann. Phys., NY* **21** 494
Ghosh A and Chakravorty D 1989 unpublished
Holstein T 1959 *Ann. Phys., NY* **24** 305
Komatsu T, Imai K, Sata R, Matusita K and Yanashita T 1988 *Japan. J. Appl. Phys. Lett.* **27** L533
Long A R 1982 *Adv. Phys.* **31** 553
Maeda H, Tanana Y, Fukutomi M and Asano T 1988 *Japan. J. Appl. Phys. Lett.* **27** L209
Mott N F 1968 *J. Non-Cryst. Solids* **1** 1
Mott N F 1969 *Phil. Mag.* **19** 835
Mott N F and Davis E A 1979 *Electronic Processes in Non-Crystalline Materials* (Oxford: Clarendon) 2nd edn
Pike G E 1972 *Phys. Rev.* B **6** 1572
Pollak M 1965 *Phys. Rev.* **138** 1822
—— 1971 *Phil. Mag.* **23** 519
Pollak M and Geballe T H 1961 *Phys. Rev.* **122** 1742
Pool R 1988 *Science* **240** 25
Sayer M and Mansingh A 1972 *Phys. Rev.* B **6** 4629
Schnakenberg J 1968 *Phys. Status Solidi* **28** 623
Sheng Z Z and Herman A M 1988 *Nature* **332** 138
Tarascon J M, Le Page Y, Barboux P, Bagley B G, Greene L H, Mekinnon W R, Hull G W, Giroud M and Hwang D M 1988 *Phys. Rev.* B **37** 9382
Wu N K, Ashburn J R, Torng C J, Hor P H, Meng R L, Gao L, Huang Z J, Wang Y Q and Chu C W 1987 *Phys. Rev. Lett.* **58** 908

Zheng H, Chen K C and Mackenzie J D 1988 *Extended Abstracts: High Temperature Superconductors II* ed. D W Capone II, W H Butler, B Batlogg and C W Chu (Pittsburgh: Materials Research Society) vol EA-14 page 93

Zheng H and Mackenzie J D 1988 *Phys. Rev.* B **38** 7166